

# Probing Resistance to Protein Adsorption of Oligo(ethylene glycol)-Terminated Self-Assembled Monolayers by Scanning Force Microscopy

K. Feldman,<sup>†</sup> G. Hähner,<sup>\*,‡</sup> N. D. Spencer,<sup>†</sup> P. Harder,<sup>‡</sup> and M. Grunze<sup>\*,‡</sup>

Contribution from the Laboratory for Surface Science and Technology, Department of Materials, ETH Zürich, Sonneggstrasse 5, CH-8092 Zürich, Switzerland, and Angewandte Physikalische Chemie, Universität Heidelberg, INF 253, 69120 Heidelberg, Germany

Received April 1, 1999

**Abstract:** Functionalized scanning force microscope (SFM) probes were used to investigate and to mimic the interaction between fibrinogen and self-assembled monolayers (SAMs) of methoxytri(ethylene glycol) undecanethiolates  $-S(CH_2)_{11}(OCH_2CH_2)_3OCH_3$  (EG3-OMe) on gold and silver surfaces. The SAMs on gold are resistant to protein adsorption, whereas the films on silver adsorb variable amounts of fibrinogen. Experiments were performed with both charged and hydrophobic tips as models for local protein structures to determine the influence of these parameters on the interaction with the SAMs. A striking difference between the two monolayers was established when the forces were measured in an aqueous environment with hydrophobic probes. While a long-range attractive hydrophobic interaction was observed for the EG3-OMe on silver, a repulsive force was measured for EG3-OMe on gold. The strong dependence of the repulsive force for the EG3-OMe-gold system upon the solution ionic strength suggests that this interaction has a significant electrostatic contribution. The observed differences are attributed to the distinct molecular conformations of the oligo(ethylene glycol) tails on the gold-supported (helical) and silver-supported (“all-trans”) monolayers. A comparison of the force/distance curves for the EG3-OMe SAMs with those measured under identical conditions on end-grafted poly(ethylene glycol) (PEG 2000) on gold further emphasizes that the nature of the repulsive forces originating from the short-chain oligomers is unique and not related to a “steric repulsion” effect.

## Introduction

Self-assembled monolayers (SAMs) of alkanethiolates on metal surfaces constitute a class of molecular assemblies formed by the spontaneous chemisorption of long-chain functionalized molecules on the surface of solid substrates.<sup>1,2</sup> Due to their ease of preparation, long-term stability, controllable surface chemical functionality, and high, crystal-like, two-dimensional order, SAMs represent suitable model surfaces to study molecular adsorption, adhesion, wetting, lubrication, and the interaction of proteins and cells with artificial organic surfaces. The latter phenomena are of crucial importance to the fields of biomaterials, biosensors, and medical devices.

The outstanding protein-resistant properties of poly(ethylene glycol) (PEG)-containing surfaces have been recognized for a long time and extensive experimental and theoretical work has been carried out to elucidate the physics underlying these properties.<sup>3–5</sup> When interpreted in terms of the “steric repulsion” theory,<sup>3–5</sup> the protein resistance of PEG is associated with a high conformational freedom and hence entropy of its solvated

chains in the near-surface region. This theory is not appropriate, however, to explain the observation that protein resistance is also inherent in oligo(ethylene glycol)-terminated alkanethiol SAMs,<sup>6</sup> where the conformational freedom of the OEG tails is restricted by packing forces.

The protein adsorption characteristics of the methoxytri(ethylene glycol) undecanethiolate (EG3-OMe) SAMs are strongly sensitive to the substrate used.<sup>7</sup> While the monolayers self-assembled on Au are protein resistant, those self-assembled on Ag are not. Fourier transform infrared reflection–absorption spectroscopic (FTIRAS) experiments show that the SAMs on Au and Ag differ in the conformation of the OEG tail.<sup>7</sup> On gold a conformation with spectral characteristics typical of helical and amorphous PEG is found, whereas the spectra observed on the Ag substrates resemble those for the planar all-trans conformation of stretched PEG samples (Figure 1). The different conformation and higher packing density in the Ag-supported monolayer is due to the formation of an incommensurate solid phase with nearly upright chains and a perceptibly smaller lattice spacing, as confirmed by calculation of the lowest-energy monolayer configurations on Au and Ag.<sup>8</sup> Good agreement is found between the experimental and calculated vibrational spectra of the lowest-energy SAM configurations on Au and Ag using our structural models.<sup>9</sup>

\* Corresponding authors.

<sup>†</sup> ETH Zürich.

<sup>‡</sup> Universität Heidelberg.

(1) Ulman, A. *Chem. Rev.* **1996**, *96*, 1533–1554.

(2) Ulman, A. *An Introduction to Ultrathin Organic Films: From Langmuir–Blodgett to Self-Assembly*; Academic Press: Boston, 1991.

(3) Harris, J. M. *Poly(Ethylene Glycol) Chemistry*; Plenum: New York, 1992.

(4) Jeon, S. I.; Andrade, J. D. *J. Colloid Interface Sci.* **1991**, *142*, 159–166.

(5) Taunton, H. J.; Toprakcioglu, C.; Fetters, L. J.; Klein, J. *Nature* **1988**, *332*, 712–714.

(6) Prime, K. L.; Whitesides, G. M. *J. Am. Chem. Soc.* **1993**, *115*, 10714–21.

(7) Harder, P.; Grunze, M.; Dahint, R.; Whitesides, G. M.; Laibinis, P. E. *J. Phys. Chem. B* **1998**, *102*, 426–436.

(8) Pertsin, A. J.; Grunze, M.; Garbuzova, I. A. *J. Phys. Chem. B* **1998**, *102*, 4918–4926.

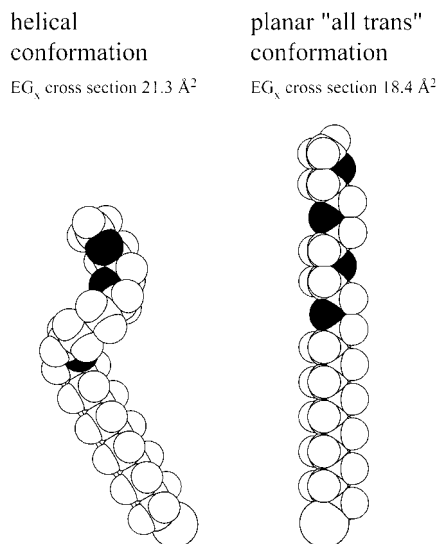


**Figure 1.** Molecular cross-sections for the helical EG3-OME on gold with a  $\sim 30^\circ$  tilt of the alkyl chain and a perpendicular orientation of "all-trans" EG3-OME on silver. For details see ref 7.

To interpret the protein-resistance properties of the SAMs containing the helical conformers, the presence of a stable interphase water layer preventing the SAM from direct contact with protein molecules was postulated from *ab initio* 6-31G SCF calculations of the microscopic structure of the SAM/water interphase region.<sup>10</sup> The observed difference in protein adsorption between the helical and planar SAM phases is assumed to be caused by a difference in the structural organization of water near the SAM surface. Calculations show that the helical SAM phase easily accommodates water molecules, which act as a template for further adsorption of water via a hydrogen bonding network. The resulting interphase water layer is tightly bound to the helical or amorphous SAM surface, thereby preventing direct contact between the surface and the protein. In contrast, the denser SAM phase on silver does not allow water molecules to form strong hydrogen bonds with oxygen atoms in the EG3-OME strands. As a result, no interphase water layer capable of hindering protein adsorption is formed. Similar explanations have been given in the literature<sup>11</sup> to correlate the inertness of some hydrophilic surfaces toward protein adsorption with the contact angles of water.

Force measurements have been performed with scanning probe techniques to study protein properties and protein-surface interactions. Apart from specific recognition and specific interactions,<sup>12–18</sup> single-molecule force spectroscopy,<sup>19</sup> adhesion forces between ligand-receptor pairs,<sup>20,21</sup> and protein adsorption

(9) Pertsin, A. J.; Grunze, M. *Langmuir* **1994**, *10*, 3668–74.

(10) Wang, R. L. C.; Kreuzer, H. J.; Grunze, M. *J. Phys. Chem. B* **1997**, *101*, 9767–9773.

(11) Vogler, E. A. *Adv. Colloid Interface Sci.* **1998**, *74*, 69–117.

(12) Florin, E. L.; Moy, V. T.; Gaub, H. E. *Science* **1994**, *264*, 415.

(13) Ludwig, M.; Moy, V. T.; Rief, M.; Florin, E. L.; Gaub, H. E. *Microsc. Microanal. Microstruct.* **1994**, *5*, 321.

(14) Lee, G. U.; Kidwell, D. A.; Colton, R. J. *Langmuir* **1994**, *10*, 354–357.

(15) Florin, E. L.; Rief, M.; Lehmann, H.; Ludwig, M.; Dornmair, C.; Moy, V. T.; Gaub, H. E. *Biosens. Bioelectron.* **1995**, *10*, 895–901.

(16) Allen, S.; Chen, X. Y.; Davies, J.; Davies, M. C.; Dawkes, A. C.; Edwards, J. C.; Roberts, C. J.; Sefton, J.; Tendler, S. J. B.; Williams, P. M. *Biochemistry* **1997**, *36*, 7457–7463.

(17) Chowdhury, P. B.; Luckham, P. F. *Colloids Surf. A* **1998**, *143*, 53–57.

(18) Bowen, W. R.; Hilal, N.; Lovitt, R. W.; Wright, C. J. *J. Colloid Interface Sci.* **1998**, *197*, 348–352.

(19) Rief, M.; Oesterhelt, F.; Heymann, B.; Gaub, H. E. *Science* **1997**, *275*, 1295–1297.

onto polymer surfaces<sup>22</sup> have also been reported in the literature. However, the importance of the different chemical regions (neutral or charged) in a protein with respect to the net interaction of the macromolecule with a surface is still being debated.<sup>23</sup>

In the following, we first describe force-distance measurements between fibrinogen-modified probes and the surfaces of tri(ethylene glycol) (EG3-OME)-terminated alkanethiolate monolayers on gold and silver, obtained with a commercial AFM to demonstrate the good correlation between these experiments and fibrinogen adsorption data obtained by FTIR. Subsequently, results obtained with charged (oxidized/hydroxylated) or hydrophobized (hexadecanethiol-derivatized) probes are reported. These experiments are conducted to elucidate qualitatively the different contributions and relevance of charged or hydrophobic patches in fibrinogen (the protein used in this study) to the resulting interactions with tri(ethylene glycol)-terminated SAMs on gold or silver.

## Experimental Section

**Materials.** EG3-OME (1-mercaptoundec-11-yl)tri(ethylene glycol) methyl ether was prepared according to a general procedure developed by Prime and Whitesides.<sup>6</sup> 11-Bromoundec-1-ene was added dropwise to a solution of tri(ethylene glycol) methyl ether in THF with 2 equiv of NaH and the solution was stirred overnight. Nonconsumed NaH was reacted with 2-propanol. The solvent was removed and the remaining product was purified by column chromatography. A solution of the olefin in methanol containing 4 equiv of thioacetic acid and 10 mg of AIBN was irradiated for 6 h under an atmosphere of nitrogen with a 450 W, medium-pressure mercury lamp. Concentration of the reaction mixtures by rotary evaporation at reduced pressure followed by purification by chromatography on silica gel gave the thioacetate. The latter was refluxed overnight in 0.5 M HCl in methanol and the concentrated solution was purified by column chromatography. The purity of the thiol was checked with NMR and mass spectroscopy. The syntheses of EG6-OH and EG[3,1]-OME have been described elsewhere.<sup>24</sup> (1-Mercaptoundec-11-yl)poly(ethylene glycol) methyl ether (MW 2000) was prepared analogous to a general procedure for mercaptoundecyl oligo(ethylenglycol) described by Prime and Whitesides.<sup>24</sup> The following changes were made: PEG 2000 monomethyl ether as starting material was dried over molecular sieve 48 h before use. For the coupling reaction to the alkyl chain, 2 equiv of 11-bromoundec-1-ene was added to a solution of PEG 2000 monomethyl ether in dry THF with 2 equiv of NaH and the mixture was stirred overnight. Purification of the different synthetic steps was carried out by column chromatography on silica gel with chloroform/methanol 1:3 as eluent. Purity and molecular weight distribution of the thiol were checked by NMR and MALDI mass spectrometry ( $M_n$  (number average) = 2199,  $M_w$  (weight average) = 2224;  $M_w/M_n$  = 1.01).

**SAM Preparation.** Polycrystalline gold (99.99%, Balzers Materials, Liechtenstein) and silver (99.99%, Aldrich Chem. Co., Milwaukee, WI) substrates were prepared by thermal evaporation of these metals onto plasma-cleaned pieces of singly polished silicon (100) wafers (MEMC Electronic Materials, Inc., St. Peters, MO) in a BAL-TEC (Balzers, Liechtenstein) MED-020 coating system operated at  $(3-5) \times 10^{-5}$  mbar. Evaporation of a 5-nm chromium adhesion layer was followed by deposition of a 100-nm layer of gold or silver at a rate of 0.5 nm/s. Coated substrates were immediately immersed into 2 mmol thiol solutions in ethanol. Upon removal from the thiol solution, the SAMs were rinsed with pure ethanol and dried with nitrogen.

(20) Lee, G. U.; Chrisey, L. A.; Colton, R. J. *Science* **1994**, *266*, 771.

(21) Moy, V. T.; Florin, E. L.; Gaub, H. E. *Colloids Surf. A* **1994**, *93*, 343.

(22) Chen, X.; Davies, M. C.; Roberts, C. J.; Tendler, S. J. B.; Williams, P. M.; Davies, J.; Dawkes, A. C.; Edwards, J. C. *Langmuir* **1997**, *13*, 4106–4111.

(23) Horbett, T. A.; Brash, J. L.; Horbett, T. A.; Brash, J. L., Eds. *American Chemical Society: Washington, DC, 1995; pp 11–14.*

(24) Prime, K. L.; Whitesides, G. W. *J. Am. Chem. Soc.* **1991**, *113*, 12.

Characterization of SAMs involved static water-contact-angle measurements with a contact-angle goniometer (Ramé-Hart, Inc., Mountain Lakes, NJ) and film-thickness measurements by ellipsometry (Type L-116C, Gaertner Science Corp., Chicago, IL) with a 70° angle of incidence of a He–Ne laser. Results of water-contact-angle measurements were in agreement with those reported earlier:<sup>7</sup> 63° ± 2° for the EG3-OMe SAMs on both gold and silver. Representative films were checked by FTIR with respect to their overall quality and molecular conformation.

A sample of PEG 2000-thiolate was prepared by immersion of a gold substrate into an ethanolic 1 mmol thiol solution for 48 h; characterization of the sample revealed that the packing density of the molecules (distance between the binding sites) is slightly less than the unperturbed radius of gyration for the given molecular weight distribution ( $R_g \sim 3.6$  nm).

**Probes for SFM Measurements.** It is known that formation of fibrinogen clusters on a hydrophobic surface is due to strong intermolecular interactions. These appear to be less significant in the presence of a mica surface.<sup>25,26</sup> Hence, to avoid clustering, we decided to mainly use oxygen-plasma-treated Si<sub>3</sub>N<sub>4</sub> probes to adsorb fibrinogen. Similarly to mica, these probes acquire a negative charge at neutral pH. It should be noted, however, that similar results to those reported in the following were also obtained using hydrophobic (C16-functionalized) probes with adsorbed fibrinogen.

“Hydrophobic” probes (referred to below as C16-probes) were prepared by vapor-phase deposition of hexadecanethiol (Aldrich Chemical Co., Inc., Milwaukee, WI) onto gold-coated Si<sub>3</sub>N<sub>4</sub> probes (Digital Instruments, Inc., Santa Barbara, CA) with a nominal radius of curvature of 30 nm. Both sides of the plasma-cleaned probes were coated with a 5-nm chromium layer followed by 50 nm of gold. After gold deposition, the probes were placed in a metal desiccator containing 200 mL of hexadecanethiol, the desiccator was then evacuated to ~0.1 mbar and kept under vacuum overnight. To ensure the quality of SAMs, a piece of a silicon wafer was gold coated and functionalized together with the probes and analyzed by ellipsometry, static contact angle, and XPS. The analyses did not reveal any notable differences between the SAMs of hexadecanethiol prepared via vapor-phase deposition and those prepared by immersion into a 5 mM solution in ethanol and therefore we assume a similar quality of the films on the Au-coated Si<sub>3</sub>N<sub>4</sub> tips used in our force measurements.

Adsorption of fibrinogen onto SFM probes was conducted according to the following protocol: Si<sub>3</sub>N<sub>4</sub> probes, previously cleaned with water-enriched oxygen plasma, or C16-probes (Digital Instruments, Inc., Santa Barbara, CA) were placed in phosphate-buffered saline solution (PBS) containing 0.01 M phosphate buffer, 0.0027 M KCl, and 0.137 M NaCl (solution obtained by dissolving PBS tablets, P-4417, Sigma Chem. Co., St. Louis, MO). Fraction I fibrinogen from human plasma (F-4883, Sigma Chem. Co., St. Louis, MO) was dissolved in PBS solution at a concentration of 2 mg/mL. This solution was then added to that containing SFM probes to achieve a final concentration of fibrinogen of approximately 1 mg/mL. After 1 h of adsorption, more PBS solution was added, followed by aspirating the liquid with a vacuum line to remove any fibrinogen film that may have formed at the liquid–air interface. This procedure was repeated several times, to ensure that upon removal of the probes from the solution no fibrinogen film was transferred from the air/water interface onto the probes.

Each set of samples was measured with only one probe to ensure that observed changes in the tip–surface interaction were not due to variability in cantilever stiffness or probe-tip radius, although the latter might be affected by the number of loading–unloading cycles. The force–distance measurements with the fibrinogen-adsorbed probes were conducted in the following manner: at least 64 force–distance curves were collected in PBS solution, both at the same point and at adjacent locations.

To gain further insight into the nature of the distinctly different protein-resistance behavior of the two monolayers, we employed probes with better-defined surface compositions to “mimic” the nonspecific interaction of the fibrinogen macromolecule with monolayers of EG3-OMe. Since proteins contain both hydrophobic and charged domains,<sup>27</sup> we used hydrophobic (C16) and oxygen-plasma-treated Si<sub>3</sub>N<sub>4</sub> probes, which acquire a net negative charge at biologically relevant pH values.

To obtain charged SFM probes we used “sharpened” Si<sub>3</sub>N<sub>4</sub> Microlevers (Park Scientific Instruments, Sunnyvale, CA) with a nominal radius of curvature of 20 nm, and treated them for 45–60 s in a RF-plasma cleaner (Harrick Scientific Corp., Ossining, NY), operated at 40 W with a water-enriched oxygen feed to ensure both removal of contaminants and hydroxylation of the probe-tip surface. The plasma-treated tips were stored either in deionized water or in PBS buffer solution.

The largest dimension of a fibrinogen molecule in the native state is on the order of 470 Å.<sup>25,28</sup> The size of the charged αC-domains of this protein and of its hydrophobic D-domains is quite comparable to the contact area between the SFM probes and the surface.<sup>28</sup>

**SFM Measurements.** Force–distance measurements and imaging were performed with a Nanoscope IIIa scanning force microscope (Digital Instruments, Inc., Santa Barbara, CA) equipped with a liquid cell. We monitored the temperature inside the cell with a K-type thermocouple. The temperature was in the range of 27–30 °C during our measurements. Force–distance curves were collected with a cycle frequency of 0.3–0.5 Hz. All liquids introduced into the liquid cell were filtered with 0.22 μm “millex-GV”, low-protein-binding filters (Millipore, Bedford, MA). Manufacturer-provided nominal values of the cantilevers’ spring constants,  $k_0$ , and frequencies,  $\omega_0$ , were used to calculate the actual spring constant,  $k$ , by measuring resonant frequencies,  $\omega$ , of the probes according to the equation:

$$k = k_0 * (\omega/\omega_0)^2$$

assuming that the effective mass of the cantilevers is constant. Prior to force-versus-distance measurements, 100- and 500-nm z-calibration gratings (TGZ-type, NT-MDT, Zelenograd, Russia) were scanned in contact mode to ensure proper calibration of the z-piezo. Piezo-displacement cantilever-deflection curves were converted into force–distance curves according to the procedure described in ref 29. Zero separation corresponds to a hard-wall potential, i.e., there is no absolute measure for the distance between tip and surface. Force-versus-distance measurements of each series of samples were performed with the same probe to minimize the error in distance due to variability in the spring constant value. It is important to note that only semiquantitative analysis of the force–distance data is possible due to the unknown precision of spring-constant and probe radii values. In addition, the probe radius may change due to blunting caused by many repetitions of the measurements.

## Results

In establishing possible differences between the EG3-OMe SAMs on gold and silver, we first recorded 3 × 3 μm<sup>2</sup> SFM images of the two surfaces in TappingMode with a 5% reduction in the set-point amplitude. A surface-roughness analysis revealed no significant differences between the root-mean-square (RMS) roughness values of the two surfaces, which were both found to be around 1.6 nm. Hence, the differences in the force–distance curves on gold and silver described below cannot be related to differences in surface topography.

Figure 2 shows representative force–separation curves measured with a fibrinogen-modified probe in pure PBS solution on a series of surfaces including mica (Figure 2a), hexadecanethiol-covered gold (Figure 2b), a protein-resistant EG3-OMe monolayer on gold (Figure 2c), and a protein-adsorbing film on silver (Figure 2d). According to FTIR measurements, the latter adsorbed about 20% of a fibrinogen monolayer.

(25) Erlandsson, R.; Olsson, L.; Bongrand, P.; Claesson, P. M.; Curtis, A. S. G., Eds.; Springer: Berlin, 1994, Chapter 4.

(26) Ta, T. C.; Sykes, M. T.; McDermott, M. T. *Langmuir* **1998**, *14*, 2435–2443.

(27) Andrade, J. D.; Horbett, T. A.; Brash, J. L., Eds. ACS Symp. Series No. 343; American Chemical Society: Washington, DC, 1987; Chapter 1.

(28) Feng, L.; Andrade, J. D.; Horbett, T. A.; Brash, J. L., Eds. ACS Symp. Series No. 602; American Chemical Society: Washington, DC, 1995; Chapter 5.

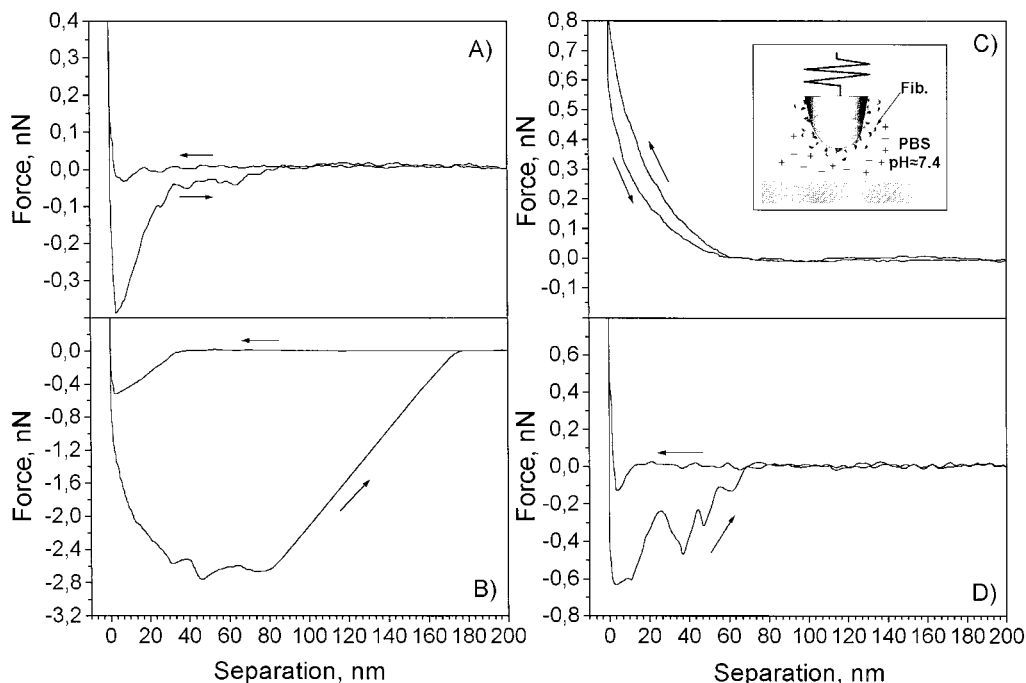


**Figure 2.** Representative force-versus-separation curves obtained with a fibrinogen-modified  $\text{Si}_3\text{N}_4$  probe ( $k = 0.03$  N/m) in PBS solution on (a) freshly cleaved mica surface, (b) hexadecanethiol SAM on gold, (c) EG3-OME SAM on gold, and (d) EG3-OME on silver showing attractive interaction and multiple pull-offs (representative of 20% of the force–distance data taken).

The hydrophilic (mica) and the hydrophobic (C16) surfaces are intended to serve as a reference for strong fibrinogen binding. Both surfaces show an attractive interaction with the fibrinogen-modified probe upon approach and strong adhesion upon retraction, indicating that the proteins establish contact to both probe and sample surfaces. Note the difference in the extent of the attractive interaction of fibrinogen between the two surfaces. Clearly, the attractive force upon approach, the pull-off forces, and the adhesion hysteresis (the area between the approaching and retracting curves) were all greatest for the fibrinogen–C16 system, which is in good agreement with results reported in the literature.<sup>26</sup>

As can be seen in Figure 2c, there are no attractive forces between a fibrinogen-modified probe and an EG3-OME monolayer on gold. However, there is a reproducible loading–unloading hysteresis, which did not change when pure buffer was replaced by fibrinogen solution. Two hundred and fifty six force curves consecutively recorded in pure PBS and fibrinogen solution gave no evidence of attractive or adhesive forces. This was reproduced on several samples.

Similar observations have been reported by Sheth and Leckband by means of a surface forces apparatus.<sup>30</sup> These authors, however, measured an attractive interaction after *pressing* streptavidin onto PEG. The very small attractive forces found in their experiment might also be present here, but the effect is too small to be unambiguously detected.

For the EG3-OME monolayer on silver, we observed multiple pull-off events indicating adhesion of the fibrinogen-coated probe, in agreement with the FTIR protein-adsorption measurements (Figure 2d).

Measurements with oxygen-plasma-treated probes were performed in air, deionized water, and the same PBS buffer as used in the protein-adsorption experiments. Force-versus-distance curves in air with an oxygen-plasma-treated probe ( $k = 0.03$  N/m) revealed no significant differences between the EG3-OME SAMs on gold and silver. A large adhesion hysteresis primarily due to capillary forces<sup>31</sup> was found for both surfaces. Pull-off

forces for the SAM were determined to be  $11.7 \pm 1.4$  nN on gold and  $10.6 \pm 0.3$  nN on silver. The broader distribution of the pull-off forces from the EG3-OME on gold might be due to the variations of the elastic modulus of the SAM on gold, which would, in turn, depend on the degree of crystalline order in the monolayer. The similarity of the pull-off forces on gold and silver in air measured with hydrophilic, largely hydroxylized probes is consistent with the similar water contact angles measured for the two monolayers.<sup>7</sup> Similar water-contact angles correspond to similar surface interfacial energies with water and, therefore, to similar values of the work of adhesion which, in turn, is reflected in the pull-off forces.

Force-versus-distance measurements were also performed with an oxygen-plasma-treated  $\text{Si}_3\text{N}_4$  probe ( $k = 0.01$  N/m) in deionized (DI) water ( $18.2$  M $\Omega$ ·cm) and PBS buffer (Figure 3). We previously found<sup>32</sup> that probes treated with water-rich oxygen plasma have an isoelectric point at  $\text{pH} \approx 3$ , which implies that at higher pH values the probes acquire a negative surface charge due to deprotonation of hydroxyl groups. Our measurements of the EG3-OME SAMs on gold and silver in DI water with a negatively charged probe showed a long-range repulsion followed by a short-range attraction, similar to a DLVO-type interaction.<sup>33</sup> The repulsive force was found to be stronger for the SAM on gold, while the pull-off forces were greater for that on silver. Measurements in PBS buffer did not reveal any significant differences between the two surfaces. As expected, the ion concentration had a significant effect on the observed interaction: for both surfaces attractive forces are observed in

(29) Ducker, W. A.; Senden, T. J.; Pashley, R. M. *Nature* **1991**, 353, 239.

(30) Sheth, S. R.; Leckband, D. *Proc. Natl. Acad. Sci.* **1997**, 94, 8399–8404.

(31) Grigg, D. A.; Russel, P. E.; Griffith, J. E. *J. Vac. Sci. Technol. A* **1992**, 10, 680.

(32) Feldman, K.; Tervoort, T.; Smith, P.; Spencer, N. D. *Langmuir* **1998**, 14, 372–378.

(33) Israelachvili, J. *Intermolecular and Surface Forces*, 2nd ed.; Academic Press: San Diego, CA, 1992.

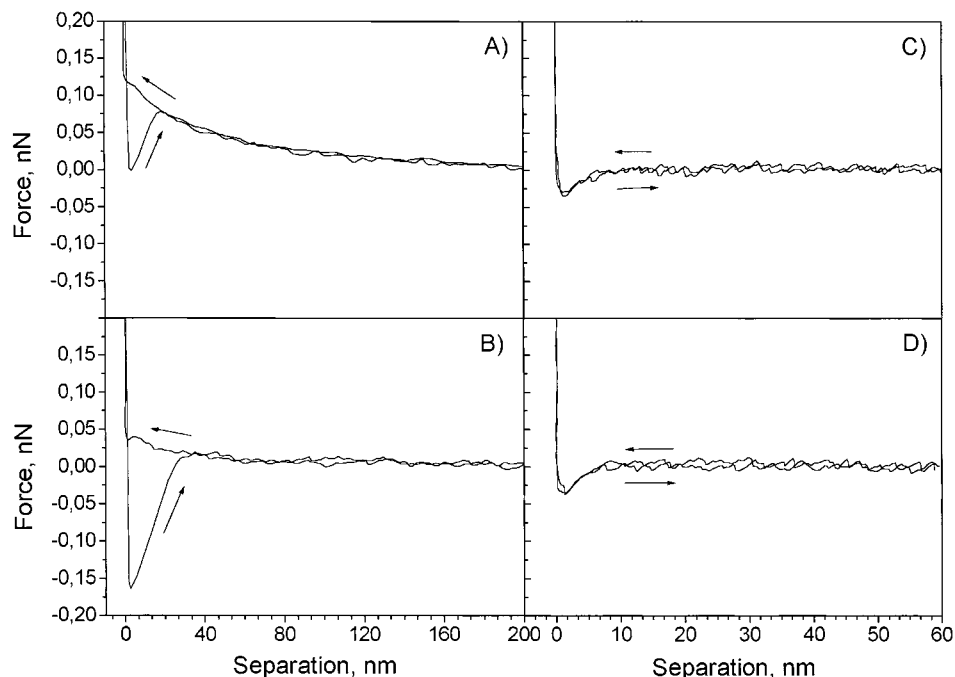


**Figure 3.** Representative force-versus-separation curves obtained with an oxygen plasma-treated  $\text{Si}_3\text{N}_4$  probe ( $k = 0.02 \text{ N/m}$ ) measured on (a) EG3-OMe on gold in deionized water, (b) EG3-OMe on silver in deionized water, (c) EG3-OMe on gold in PBS solution, and (d) EG3-OMe on silver in PBS solution.

the PBS experiment, with a significantly smaller range of interaction compared to measurements in DI water.

The most interesting results were obtained with hydrophobic probes. Measurements in pure water with C16-probes revealed a long-range repulsion for the EG3-OMe monolayer on gold and a long-range attraction for that on silver (Figure 4). When DI water was replaced by PBS solution, the extent of the repulsive interaction diminished on gold, but did not change sign. For silver, however, only very small changes were found in PBS buffer as compared to pure water (Figure 4). The experiments were repeated many times with different samples of EG3-OMe and several batches of C16-probes to confirm their correlation with the FTIR protein-adsorption measurements. We also investigated two other 1-undecylthiols, either with a hydroxyl-terminated hexa(ethylene glycol) (EG6-OH) or a methoxy-terminated tri(ethylene glycol) (EG3-OMe) end group and a  $-\text{CH}_2\text{OCH}_3$  side chain at the C-12 atom (EG[3,1]-OMe). Force-distance measurements on monolayers of either thiol on gold or silver established the same correlation for all investigated films. Whenever a repulsive force was observed upon approach of a *hydrophobic* probe in PBS solution, that surface resisted fibrinogen adsorption as determined by the FTIR measurements.

The repulsive curves measured upon approach to EG3-OMe on gold showed some variability with respect to the range of interaction. Some of them were purely repulsive, while occasionally a jump-to-contact at distances of  $\sim 5 \text{ nm}$  before contact appeared. Whenever a jump-to-contact occurred, this was accompanied by a hysteresis in the loading-unloading cycle, while no hysteresis was found in the purely repulsive curves. This variability of the SFM data in terms of the *range* of the forces and the presence of an adhesion hysteresis might be attributed to the structural inhomogeneity of the monolayers, i.e., the presence of different phases with dissimilar mechanical properties in the EG3-OMe layer.

Force-distance measurements with a C16-probe and an EG3-OMe SAM on gold in DI water and PBS solution revealed a strong dependence of the range of the repulsive force upon the ionic strength of the solution; the same measurements for the

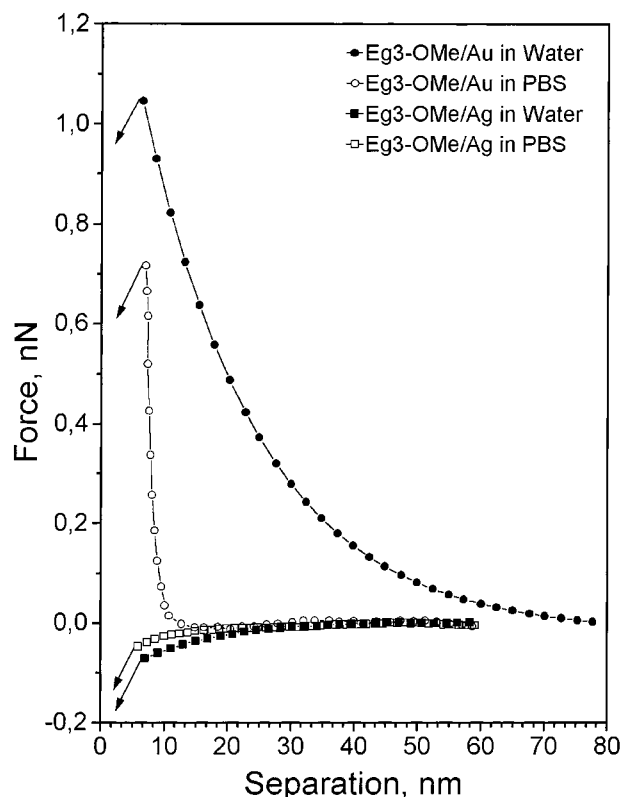


**Figure 4.** Advancing force-versus-separation curves measured with a hydrophobic C16-probe ( $k = 0.12 \text{ N/m}$ ) in deionized water and PBS solution on the SAMs of EG3-OMe on gold and silver.

monolayer on silver showed a long-range attractive interaction with very little dependence on the ionic strength. These results suggest that, due to different conformations of the EG3-OMe molecules on gold and silver, the observed interactions may well be of a distinct physical nature, i.e., electrostatic for EG3-OMe on gold and hydrophobic for that on silver. To further elucidate this hypothesis, we performed force-distance mea-

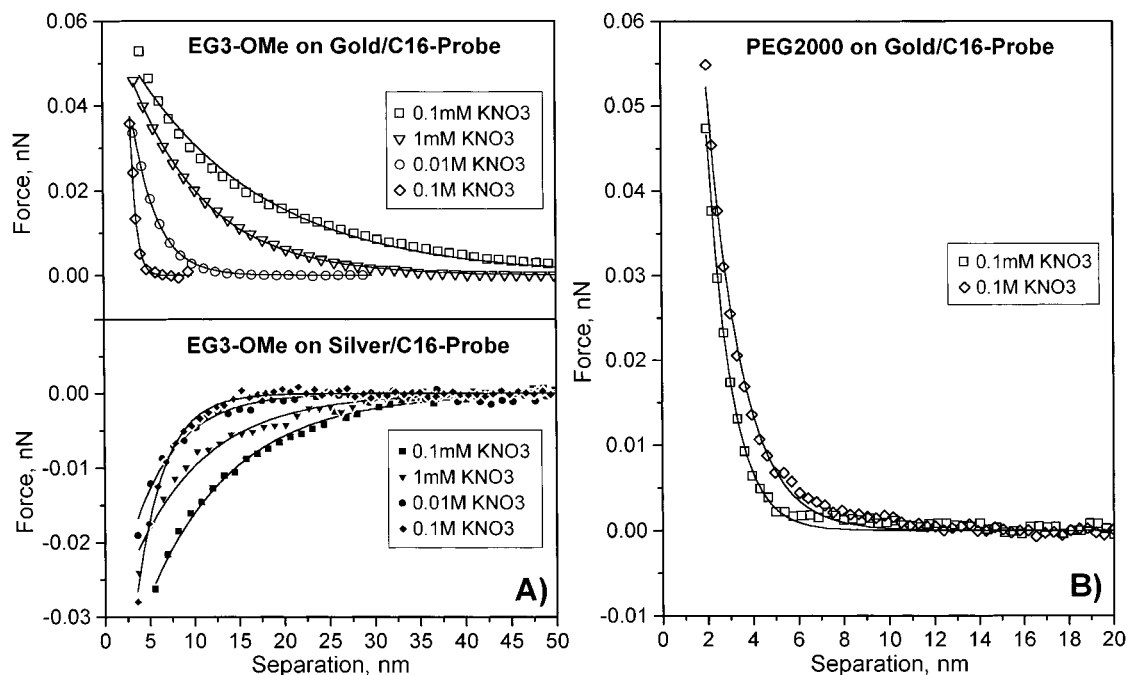


**Figure 5.** Advancing force-versus-separation curves measured with a hydrophobic C16-probe ( $k = 0.06$  N/m) in aqueous solutions of  $\text{KNO}_3$  on (a) the SAMs of EG3-OMe on gold and silver and (b) PEG2000-thiolate on gold. Solid lines represent fitted data.

measurements with a C16-probe on the two monolayers in aqueous solutions of  $\text{KNO}_3$  of various ionic strengths (Figure 5a), and, once again, detected repulsive forces for the EG3-OMe on gold that displayed a strong dependence upon the ionic strength of the solution and attractive long-range forces for that on silver that were less influenced by the presence and concentration of ions.

We also performed measurements on the end-grafted PEG 2000 brush on gold with a C16-probe (Figure 5b) to demonstrate that the long-range effects observed on packed, ordered monolayers of EG3-OMe are not detected in grafted polymer brushes. Also, in marked contrast to the behavior of the shorter molecules, end-grafted PEG scarcely revealed any ionic-strength dependence.

According to previous theoretical work on these systems,<sup>10</sup> strong interaction of water molecules with the helical conformer of the EG3-OMe SAM on gold is a necessary condition for protein resistance, because oligo(ethylene glycol) per se is not intrinsically protein resistant. Water cannot associate with the all-trans structure of the EG3-OMe SAM on silver, and hence this system exhibits protein-adsorption behavior that is characteristic for a slightly hydrophobic surface. To demonstrate unambiguously that the solvent plays a crucial role in explaining the difference in the adsorption characteristic of the helical and all-trans conformers, force-distance measurements with a hydrophobic probe were performed in perfluorodecalin  $\text{C}_{10}\text{F}_{18}$  (Fluorochem, U.K.), which is a nonpolar, non-hydrogen-bonding liquid with a low dielectric constant ( $\epsilon \sim 2.0$ ). In agreement with the theoretical arguments, we did not observe any long-range forces in perfluorodecalin on the two SAMs (Figure 6). Instead we found attractive interactions on both surfaces.

## Discussion

The images recorded for EG3-OMe on gold and silver did not reveal any differences in roughness. Since the protein-adsorption experiments were conducted using fibrinogen, which is known to have an extremely high surface activity,<sup>28</sup> one would not expect roughness to be a factor influencing the surface

affinity of fibrinogen. However, it is helpful to be able to exclude surface roughness as a possible variable in our experiments.

The presence of a hysteresis in the repulsive part of the force curve measured with a fibrinogen-coated C16-probe for EG3-OMe on gold (Figure 2c) indicates the presence of energy-dissipating processes, which can be attributed to viscoelastic conformational changes in the protein layer induced by the loading pressure. Although pressure-induced changes in protein conformation during loading and unloading might lead to aggregation of protein in the contact area, giving rise to long-range repulsive forces,<sup>34</sup> successive measurements at a single surface location showed no changes in the interaction. This also confirms that the protein layer recovers upon the retraction of the probe and that no plastic deformation is induced.

The interaction between charged bodies in electrolyte solutions can be described by the DLVO theory, which takes into account both electrostatic and van der Waals forces.<sup>33</sup> For low surface potentials ( $\psi < 25$  mV) the electrostatic force per unit area between the two bodies bearing charge densities  $\sigma_1$  and  $\sigma_2$  can be described by the following equation:<sup>35,36</sup>

$$F_{\text{el}} = \frac{2}{\epsilon\epsilon_0} [(\sigma_1^2 + \sigma_2^2)e^{-2\kappa D} + \sigma_1\sigma_2e^{-\kappa D}] \quad (1)$$

For larger separations, electrostatic force between a sphere of radius  $R$  and a flat surface becomes:<sup>36,37</sup>

$$F_{\text{el}} = \frac{4\pi R\sigma_1\sigma_2}{\epsilon\epsilon_0\kappa} e^{-\kappa D} \quad (2)$$

where  $1/\kappa$  is the so-called Debye length and  $D$  is the separation between the two bodies. The Debye length, being a solution property, can be calculated from the following equation:<sup>33</sup>

(34) Claesson, P. M.; Blomberg, E.; Froberg, J. C.; Nylander, T.; Arnebrant, T. *Adv. Colloid Interface Sci.* **1995**, *57*, 161–227.

(35) Parsegian, V. A.; Gingell, D. *Biophys. J.* **1972**, *12*, 1192–1204.

(36) Butt, H.-J. *Biophys. J.* **1991**, *60*, 777–785.

(37) Butt, H.-J.; Jaschke, M.; Ducker, W. *Bioelectrochem. Bioenerg.* **1995**, *38*, 191.

$$\kappa = \left( \sum_i \frac{\rho_{\text{ooj}} e^2 z_i^2}{\epsilon \epsilon_0 k_B T} \right)^{1/2} m^{-1} \quad (3)$$

where  $\rho_{\text{ooj}}$  is the bulk ionic concentration,  $z_i$  is the ionic charge,  $k_B$  is Boltzmann's constant,  $e$  is the electronic charge, and  $T$  is the absolute temperature.

One important implication of eq 1 is that the overall electrostatic interaction is not eliminated when one of the surface charge densities is set to zero, e.g.  $\sigma_1 = 0$  and  $\sigma_2 \neq 0$ . It is therefore not necessary for the both surfaces to carry charges.

The issue of surface charges on the EG3-OMe monolayer on gold is also important. The tails of EG3-OMe on gold can easily accommodate water molecules and seem to be present in both helical and amorphous states; for such "soft", permeable interfaces with polar tails it has been shown that the *effective* surface charge density,  $\sigma_{\text{eff}}$ , depends on the surface charge density,  $\sigma$ , and the dipole density,  $\nu$ :<sup>38,39,40</sup>

$$\sigma_{\text{eff}} = [\sigma \cosh(\kappa l) + \nu \kappa \sinh(\kappa l)] e^{-\kappa l} \quad (4)$$

where  $l$  is the thickness of the "soft" polar region. Therefore, if there are no surface charges (or the net surface charge is zero) but there is a dipole field, a surface would bear an effective non-zero charge, which would give rise to an electrostatic interaction.

Long-range repulsive forces followed by short-range attraction were measured in DI water for the EG3-OMe monolayers on gold and silver substrates with a negatively charged oxygen-plasma-treated  $\text{Si}_3\text{N}_4$  probe (Figure 3). When comparing the force curves in DI water and PBS buffer it becomes clear that the ion concentration has a pronounced effect on the tip/substrate interaction. The two substrates differ only in the strength of the repulsive force. This difference may be explained if we now assume that, due to conformational differences, the EG3-OMe monolayer on gold carries an effective surface charge (eq 4), while that on silver does not. There will still be a repulsive electrostatic interaction on silver (see eq 1, with  $\sigma_2 = 0$ ) but it will be weaker than that for gold where  $\sigma_1 \neq 0$  and  $\sigma_2 \neq 0$ . Upon introduction of the PBS solution, the range of the electrostatic force is, as expected, dramatically reduced. The screening of the electrostatic repulsion is due to the high ionic strength of the PBS solution (we calculated the Debye length of the PBS solution to be  $1/\kappa = 0.76$  nm at room temperature compared to  $\sim 1 \mu\text{m}$  for DI water) and only the attractive van der Waals forces are clearly observed (Figure 3). In addition, the type of interaction changed from repulsive in pure water to attractive in PBS buffer, the range was found to be much shorter in the case of high ion concentrations, and almost no hysteresis was found for measurements performed in PBS buffer, although the hysteresis might also scale with the Debye length and hence be too small to be detectable here.

The EG3-OMe monolayer on silver consists of molecules that are tightly packed and expose their hydrophobic methyl groups at the film/water interphase. The observed long-range attractive forces between the hydrophobic C16-probe and the EG3-OMe SAM on silver in water and PBS solution (Figure 4) point to the presence of hydrophobic interaction.<sup>41,42</sup> Indeed, these force curves are well reproduced by exponential fits with decay

lengths of 11 nm in pure water and 6 nm in PBS buffer (Figure 4). These are typical decay lengths for hydrophobic forces. Although the molecular origin of hydrophobic forces is not well understood<sup>43</sup> and the extent of the interaction is often questioned,<sup>44</sup> there is substantial experimental evidence of a long-range attractive interaction in an aqueous environment between hydrophobic surfaces with the attractive forces sometimes being sensed at separations of 50 nm and more.<sup>41,45</sup>

In contrast to the attractive hydrophobic interaction between EG3-OMe film on silver and the C16-probe, a strong dependence of the *repulsive* force on the ion concentration observed on the EG3-OMe monolayer on gold in DI water and PBS buffer suggests that this interaction involves a significant electrostatic contribution. Furthermore, since the helical or amorphous structure of the OEG tails of the SAM on gold allows a strong interaction of water molecules via hydrogen bonding with oxygen atoms of the OEG, there might be an additional repulsive contribution of hydration or steric-protrusion forces, which decay roughly exponentially with a distance of 0.2–0.4 nm.<sup>42,45</sup> This short-range, exponentially decaying force observed in PBS solution looks similar to data obtained on lipid bilayers in pure water with SFM<sup>46</sup> and the surface forces apparatus (SFA),<sup>47</sup> and is assigned to steric/hydration forces there.<sup>33,46,47</sup>

Study of the ionic concentration effect on the range of forces measured between the EG3-OMe SAMs and C16-probes (Figure 5a) provided further evidence that the overall interaction with the monolayer on gold had a significant electrostatic component. Data for EG3-OMe on gold shown in Figure 5a were fitted with an electrostatic force law for a case where the second surface (in our case, that of the C16-probe) does not carry a surface charge (see eq 1). Measurements of the symmetric system C16-probe/C16-surface did not show any repulsive interaction in water and salt solutions indicating that there were no charges present on these surfaces and the interaction was found to be strongly attractive and occurred at separations of about 20 nm. Note that traces of ions (in particular,  $\text{HCO}_3^-$  from dissolved  $\text{CO}_2$ ) present in the water may reduce the Debye length of dilute solutions significantly.

Although for the case of charge on one side only, eq 1 reduces to  $F_{\text{el}} \propto e^{-2\kappa D}$ , we found that for most measurements and higher ionic strengths the experimental data were best fitted with  $F_{\text{el}} \propto e^{-\kappa D}$ . We performed measurements using a C16-probe and a bare  $\text{SiO}_x$  surface in aqueous solutions of  $\text{KNO}_3$ —also a "charge-on-one-side-only" system—and also observed in this case that the data were best fitted with the  $e^{-\kappa D}$  coefficient. We believe that this is an image force effect, which comes into play for counterions in water that are surrounded by surfaces of higher dielectric constant.<sup>33</sup>

Results of the fits to the EG3-OMe data are shown in Table 1. The radius of the probe used was checked by scanning over the ridges of a  $\text{SrTiO}_3$  single crystal<sup>48</sup> and was found to be  $\sim 110$  nm. Dipole moments per molecule were calculated from dipole density,  $\nu$ , assuming  $l = 1$  nm in eq 4 and packing density of  $21.3 \text{ \AA}^2/\text{molecule}$ .<sup>7</sup> Data for EG3-OMe on silver were fitted with

(41) Yoon, R. H.; Flinn, D. H.; Rabinovich, Y. I. *J. Colloid Interface Sci.* **1997**, *185*, 363–370.

(42) Israelachvili, J.; Wennerström, H. *Nature* **1996**, *379*, 219–225.

(43) Tsao, Y.-H.; Evans, D. F.; Wennerström, H. *Science* **1993**, *262*, 547–550.

(44) Wood, J.; Sharma, R. *Langmuir* **1995**, *11*, 4797–4802.

(45) Claesson, P. M.; Bongrand, P.; Claesson, P. M.; Curtis, A. S. G., Eds. Springer: Berlin, 1994, Chapter 2.

(46) Dufřene, Y. F.; Barger, W. R.; Green, J. B. D.; Lee, G. U. *Langmuir* **1997**, *13*, 4779–4784.

(47) Marra, J.; Israelachvili, J. *Biochemistry* **1985**, *24*, 4608.

(48) Sheiko, S. S.; Möller, M.; Reuvekamp, E. M. C. M.; Zandbergen, H. W. *Phys. Rev. B* **1993**, *48*, 5675.

(38) Bell, G. M.; Levine, P. L. *J. Colloid Interface Sci.* **1980**, *74*, 530–548.

(39) Belaya, M.; Levadny, V.; Pink, D. A. *Langmuir* **1994**, *10*, 2010–2014.

(40) Xu, W.; Blackford, B. L.; Cordes, J. G.; Jericho, M. H.; Pink, D. A.; Levadny, V. G.; Beveridge, T. *Biophys. J.* **1997**, *72*, 1404–1413.

**Table 1.** Fitting Results of the Data Shown in Figure 5a

KNO <sub>3</sub> concn, M	EG3-OMe on gold			
	1/ $\kappa$ calcd, nm	1/ $\kappa$ fitted, nm	dipole moments/ molecule, D	EG3-OMe on Ag 1/ $\lambda$ , nm
10 <sup>-4</sup>	30.7	14.5	4.6	9.6
10 <sup>-3</sup>	9.7	9.3	2.5	8.3
10 <sup>-2</sup>	3.1	2.7	2.2	5.1
10 <sup>-1</sup>	1.0	0.7	1.4	3.1

empirical formula<sup>41</sup> of the form  $F_h \propto \exp(-\lambda D)$  to demonstrate that, unlike the situation on gold, the constant  $1/\lambda$  does not correlate with the calculated Debye length of the solution. Apparently, while the molecular conformers of OEG on the gold surface generate sufficiently strong dipolar fields to cause a screenable electrostatic interaction with the C16-probe, the interaction on silver is dominated by nonelectrostatic forces. A detailed discussion on the difference in dipolar moments for the helical, amorphous, and planar “all trans” conformers in contact with water will be presented elsewhere.<sup>49</sup>

Experiments with end-grafted PEG 2000 show a clear distinction between PEG brush behavior and that of EG3-OMe monolayers. The brushes exhibit *no long-range* interactions and little ionic strength dependence (Figure 5b). In fact, the force was found to become slightly more repulsive with increasing ionic strength, since the 0.1 M KNO<sub>3</sub> solution represents good solvent conditions.<sup>33</sup> The lack of long-range interactions for the polymer brush demonstrates that the repulsive interactions found for the short-chain oligomers is unique and not related to the steric repulsion effect responsible for the protein resistance for the end-grafted polymers.

Finally, the data recorded for EG3-OMe on Au and Ag under perfluorodecalin (Figure 6) illustrate the fact that the difference in the interfacial force does not only depend on the molecular conformation, but also on the solvent, and is significant only in an aqueous environment. Hence, to understand resistance to protein adsorption of biological or organic surfaces, it is important that the complete system, i.e., film and solvent, be considered.

## Conclusions

By means of a scanning force microscope with well-defined, functionalized tips, we were able to elucidate the contributions that are relevant to protein adsorption of fibrinogen on SAMs of EG3-OMe on gold and silver.

When using a hydrophobic tip to mimic hydrophobic regions of the protein, interactions of opposite sign were observed on the EG3-OMe-Au and EG3-OMe-Ag systems in aqueous media. While the attractive force observed on the silver system appeared

(49) Zolk, M.; Buck, M.; Eisert, F.; Grunze, M.; Wang, R.; Kreuzer, H. J. In preparation.

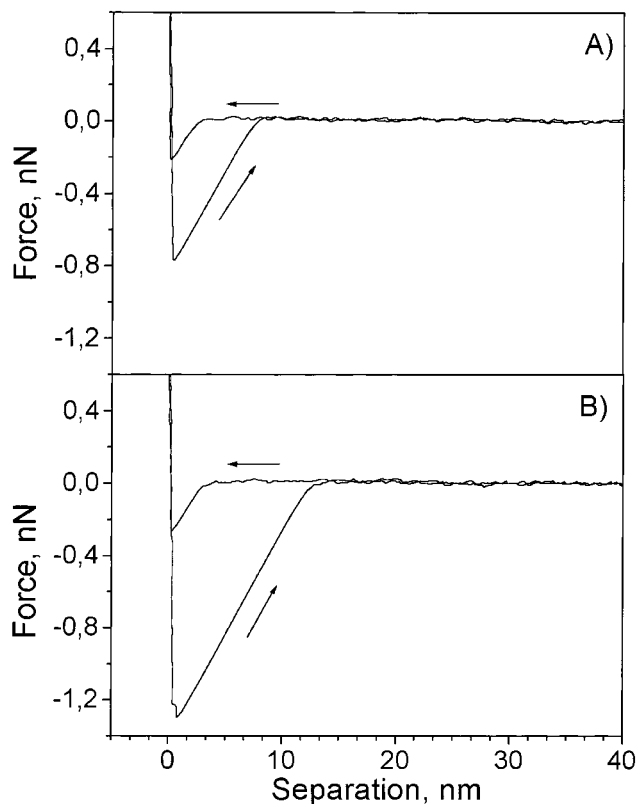


**Figure 6.** Representative force-versus-separation curves measured with the C16-probe ( $k = 0.12$  N/m) in perfluorodecalin on (a) EG3-OMe on gold and (b) EG3-OMe on silver.

to be hydrophobic in nature, the long-range repulsive force measured on the gold system displayed a strong ionic strength dependence, implying an important electrostatic component. The difference in sign of the forces can be correlated with the distinct molecular conformations of the OEG tails and the resulting difference in their dipolar fields. This effect dominates the interaction between the OEG-derivatized SAM and the SPM probe in the case of the helical and amorphous conformers on gold but is too small to contribute significantly to the total interaction in the case of the planar, “all trans” conformers on silver.

**Acknowledgment.** We thank the Deutsche Forschungsgemeinschaft, the Office of Naval Research, and the Council of the Swiss Federal Institutes of Technology (PPM and MINAST Program) for their financial support of this work. We thank W. Eck and S. Herrwerth for the EG3-OMe and PEG 2000 materials.

JA991049B